J Mol Model (2013) 19:1273–1283
DOI 10.1007/s00894-012-1659-x

ORIGINAL PAPER

Natures of benzene-water and pyrrole-water interactions in the forms of σ and π types: theoretical studies from clusters to liquid mixture

Wei Gao · Jiqing Jiao · Huajie Feng · Xiaopeng Xuan · Liuping Chen

Received: 8 August 2012 / Accepted: 21 October 2012 / Published online: 23 November 2012

Abstract A combined and sequential use of quantum mechanical (QM) calculations and classical molecular dynamics (MD) simulations was made to investigate the σ and π types of hydrogen bond (HB) in benzene-water and pyrrole-water as clusters and as their liquid mixture, respectively. This paper aims at analyzing similarities and differences of these HBs resulted from QM and MD on an equal footing. Based on the optimized geometry at ωb97xD/aug-cc-pVTZ level of theory, the nature and property of σ and π types of HBs are unveiled by means of atoms in molecules (AIM), natural bond orbital (NBO) and energy decomposition analysis (EDA). In light of the above findings, MD simulation with OPLS-AA and SPC model was applied to study the liquid mixture at different temperatures. The MD results further characterize the behavior and structural properties of σ and π types HBs, which are somewhat different but reasonable for the clusters by QM. Finally, we provide a reasonable explanation for the different solubility between benzene/water and pyrrole/water.

Keywords Cluster · Liquid mixture · Pyrrole-water and benzene-water · σ and π hydrogen bond

W. Gao · J. Jiao · H. Feng · L. Chen (✉)
KLGHEI of Environment and Energy Chemistry,
School of Chemistry and Chemical Engineering,
Sun Yat-sen University,
Guangzhou 510275, China
e-mail: cesclp@mail.sysu.edu.cn

W. Gao
College of Pharmacy, Guangdong Pharmaceutical University,
Guangzhou 510006, China

X. Xuan
School of Chemical and Environmental Sciences,
Key Laboratory of Green Chemical Media and Reactions,
Ministry of Education, Henan Normal University,
Xinxiang, Henan 453007, China

Introduction

The covalent interactions lead to the formation of a classical molecule while noncovalent interactions result in the formation of molecular clusters. The noncovalent interactions between aromatic molecules and water are believed to play an important role in chemistry and biology. Some cases include, but are certainly not limited to the conformation of protein, DNA base-pair stacking, drug-acceptor binding, organic crystal and ionic liquid. In these cases, the crucial X–H···Y hydrogen bonding (HB) interactions can be found, in which X–H acts as HB donor while Y is HB acceptor. Here, X is usually an element with higher electro-negativity than that of H (e.g., O, F or N atom), and Y is either an electro-negative atom having one or more lone electron pairs, or a region having π electron-rich such as aromatic ring [1–8], which usually denoted as X–H···π HB.

There have been many experimental [9–11] and theoretical [2–7, 12–16] investigations into various types of HBs between aromatic moiety and water. Benzene (Bz)-water (W) and pyrrole (Py)-water (W) are two interesting models because they can form different types of interactions [2, 3, 12–16]. A large number of quantum mechanical (QM) investigations have been devoted to characterizing the intricacies of benzene and water clusters [17–21]. The various microstructures and inter-molecular interactions of benzene-$(H_2O)_n$ clusters (n=1∼12) [18–21] have been explored extensively, and it has even become a common model to assess the accuracy and efficiency of newly-developed QM methods [22–24]. Additionally, the local structure of benzene in liquid water has also been studied by both experiment [25] and molecualr dynamics (MD) simulations [25–32], focusing on the structural characteristics [25–31], hydrophobic effect [31, 32] and dynamic properties of interface [26, 27]. Even in a broad range from ambient to supercritical conditions [27, 28], some anomalous behaviors of benzene-

water mixture have also been explored by MD. Compared with the model of benzene and water, there have been few experimental [33–35] and theoretical research works on the structure and interaction of pyrrole-water clusters [35–38]. Due to understanding of the electron-ejection mechanism, more attention was paid to pyrrole-$(H_2O)_n$ of excitation state rather than the ground state [35–38]. In the case of the liquid mixture of pyrrole and water, there has been several simulation studies associated with the microstructure and its excited states by means of classical [14, 15] and *ab intio* MD [36–38], respectively. For the HB contacts formed between benzene and pyrrole with water (e.g., σ-type or π-type HB [2–4]), the viewpoints derived from different theoretical methods are not completely consistent with each other. For instance, Crittenden has listed that different configurations and energies of π type HB of Bz-W have been observed using different methods [12]. Mishra found that σ type HB of Bz-W has three imaginary frequencies at the MP2/6-311++G** level, and its energy is 0.98 kcal mol^{-1} [13]. Scheiner observed the stable structure of σ type HB of Bz-W at MP2/6-31+G** with an energy of 1.1 kcal mol^{-1} [3]. The results of Kim at the B3LYP/6-311++G** and MP2/aug-cc-pVDZ levels show that σ and π types HBs of Py-W have different configurations, and the σ type is more stable than the π type at the B3LYP/6-311++G** level, but their energies are very close at the MP2/aug-cc-pVDZ level [36].

In this work, two types of HBs for both benzene-water and pyrrole-water complexes were investigated, in which benzene or pyrrole functions as either the HB donor or the acceptor. For the first type of HB of pyrrole-water complex, there is a classical N–H···O HB forming between the N–H group of pyrrole and O atom of water. While in benzene-water complex, similarly to N–H···O HB structure, a C–H···O HB may form involving the C–H group of benzene and O atom of water. This type of HBs taking the aromatic ring as HB donor and water as acceptor are referred to as X–H···O, σ-type HB. The benzene-water and pyrrole-water in the form of σ-type are denoted as BzWσ and PyWσ, respectively [3]. The second type of HB occurred between the π electronic cloud of aromatic ring and the O–H group of water. In this case, the aromatic ring as HB acceptor and water as HB donor, so the interactions are referred to as O–H···π, π-type HB, and the benzene-water and pyrrole-water are denoted as BzWπ and PyWπ, respectively [3]. To date, there are no comprehensive comparisons of these types of HBs at the same level of theory, particularly for their property, strength and origin. More importantly, when small cluster is extended to liquid phase, a question is whether such HB interactions still occur in liquid mixture. Unfortunately, neither has there been any effort in comparing differences in HBs in liquid mixture of aromatic and water on an equal footing. Therefore, it is interesting to make comparison on similarities and differences among various HBs possibly existing in pyrrole-water and benzene-water complexes, as well as those in liquid phase, which, despite a lot of experimental and theoretical effort, have still not been fully understood.

Methods

Quantum mechanical calculation

Noticeably, many studies confirmed that dispersion interaction is the major factor stabilizing in X–H···π interaction [39, 40] such as BzWπ and PyWπ. Therefore, an appropriate method is required for examining these types of HBs. The second order perturbation theory (MP2) method tends to overestimate π···π interactions and has strong basis set dependence [39], whereas general density functional theory (DFT) methods with the commonly employed functionals do not describe dispersion completely [39–42]. Nevertheless, the DFT methodology has recently developed a variety of methods to treat the dispersion interactions. Among these DFT improved approaches, the DFT-D methods [43, 44] by adding an empirical dispersion corrected term (D) has been proved to be a promising way to describe dispersion effects. As one of DFT-D methods, the ωb97xD functional which based on the ωb97 functional [45, 46] is expected to be the preferred choice for its better performance and great efficiency [39, 47, 48]. Herein, ωb97xD/aug-cc-pVTZ with correction of the basis set superposition error (BSSE) by counterpoise (CP) [49, 50] was used for the geometry optimizations of these clusters. A tight convergence criterion and ultrafine grids available in Gaussian 09 suite [51] were employed for all the optimizations in view of the flat potential energy surface (PES). In this study, all calculations of the clusters were obtained with aug-cc-pVTZ basis set, unless otherwise specified. Based on the fully optimized structures at the ωb97xD level of theory, the ωb97xD, B2PLYPD [52], M06-2X [53] and MP2 methods were used to obtain the interaction energies with correction of the BSSE by CP. All the above calculations were carried out using the Gaussian 09 suite. Atoms in molecules (AIM) analysis [54–56] was carried out at the M06-2X/aug-cc-pVTZ to characterize the topological properties of HB. The AIM was calculated with AIMAll 10.03.25 [57] and visualized via the Multiwfn 2.3.3 [58, 59] which can provide us an intuitive insight into the interaction. Natural bond orbital (NBO) analysis [60] was performed at the M06-2X/aug-cc-pVTZ, using the NBO 3.1 program included in the Gaussian 09 suite and visualizing via the Multiwfn 2.3.3. To gain a deeper insight into the nature of the two types of HB interactions, an energy decomposition analysis (EDA) proposed by Morokuma [61] and developed by Ziegler and

Rauk [62, 63] was implemented for the pyrrole-water and benzene-water complexes at the BLYP-D/TZ2P levels of theory, which has been successfully used in the study of the interactions energy for various weak interactions models [64]. The EDA analysis was performed on the program package ADF2012.01 [65]. The total interaction energy ΔE_{int}, can be expressed as Eq. (1) (if dispersion is considered):

$$\Delta E_{int} = \Delta E_{elstat} + \Delta E_{disp} + \Delta E_{pauli} + \Delta E_{orb} \quad (1)$$

Here, ΔE_{elstat} corresponds to the classical electrostatic interaction energy between the fragments calculated with the electron density distribution in the complex. ΔE_{disp} measures the dispersion energy of inter-molecules. ΔE_{pauli} denotes the repulsive interactions between the fragments, which resulted from two electrons with the same spin can not occupy the same region in space. ΔE_{orb} gives the stabilizing orbital interaction energy of the inter-atomic orbital overlapping [66–68].

Molecular dynamics simulation

The classical MD simulation [69] was performed to study the interaction of benzene and water or of pyrrole and water in liquid phase in comparison with those in the gas phase. In the classical MD simulation with optimized potentials for liquid simulations all-atom (OPLS-AA) force field [70], the molecular interactions are expressed by a sum of the Coulomb and Lennard-Jones terms as Eq. (2).

$$\Delta E_{int} = \sum_{nonbond} \left\{ q_i q_j / r_{ij} + 4\varepsilon_{ij} \left[\left(\sigma_{ij} / r_{ij} \right)^{12} - \left(\sigma_{ij} / r_{ij} \right)^{6} \right] \right\} \quad (2)$$

where the ΔE_{int} is the interaction energy between atom i and j. The first term ($q_i q_j$ / r_{ij}) is ascribed to classical electrostatic interaction and the second one $\left(4\varepsilon_{ij} \left[\left(\sigma_{ij} / r_{ij} \right)^{12} - \left(\sigma_{ij} / r_{ij} \right)^{6} \right] \right)$ to van der Waals interaction which implicitly involves the dispersion interaction. Combining rules (Berthelot rule) are used for both L-J parameters via Eq. (3):

$$\sigma_{ij} = \sqrt{\sigma_{ii}\sigma_{jj}},\ \varepsilon_{ij} = \sqrt{\varepsilon_{ii}\varepsilon_{jj}} \quad (3)$$

The MD simulation was performed with Tinker 4.2 suite [71]. The simple point charge (SPC) [72, 73] potential function was implemented for water, with the flexible mode. At the same time, the OPLS-AA we used for liquid of benzene [70] and pyrrole [74, 75]. The *NPT* ensemble was applied to the simulations in which the pressure is kept constant at 0.1 MPa and the temperatures is set at 278 K, 298 K and 318 K. The Ewald method was applied to describe long-range electrostatic interaction. All simulation systems were adopted by the 256 water molecules and 256 aromatic molecules with binary solution of 1:1 mixture, which is similar to their clusters. These simulations were sufficiently equilibrated for 5 ns to ensure that there are no systematic drifts in energies with time. The equilibrations were followed by monitoring the radial distribution function (RDF) and density. The statistics and analysis were collected during the 200 ps after equilibration.

Results and discussion

Benzene-water and pyrrole-water complexes in gas phase

Geometry and frequency

All the geometries were fully optimized at the ωb97xD/aug-cc-pVTZ level of theory with BSSE correction and no imaginary frequencies were found. In structure of BzWπ, the *R* (O···π) measured with reference to the centers of mass of benzene (n1) and O atom of water is 3.3085 Å, while corresponding experiment was 3.411 Å [17]. With respect to geometry of PyWσ, the *R* (O···N) determined as the distance between the N atom of pyrrole and O atom of water is 2.9977 Å, while corresponding experimental was 3.01–3.03 Å [33]. Unfortunately, to our best knowledge, experimental observations of the structure of BzWσ and PyWπ have not yet been reported. It can be inferred from the comparisons that the ωb97xD/aug-cc-pVTZ with BSSE correction method performs well in the prediction of structure of these clusters. We believe it also has a similar performance for predicting the structures of other clusters in this paper.

We initially highlight the major geometrical features of these clusters. As shown in Fig. 1 and Table 1, both the BzWσ and PyWσ are found to be nearly linear, the H···O distances *R*(X–H···O) decrease from 2.4892 to 1.9888 Å, respectively. By contrast BzWπ and PyWπ, the water molecule is located above the plane of benzene and pyrrole, their distances *R*(O–H···π) are 2.7191 and 2.5090 Å, respectively. Compared to the X–H bonds in its monomer, the C–H bond of BzWσ elongated slightly by 0.00031 Å, while the N–H bond of PyWσ elongated by 0.0078 Å upon complexation (see Table 1). Correspondingly, the stretching frequency ν(C–H) has a slight red-shift of 2 cm^{-1} for BzWσ (as seems to be the small red-shift [76, 77]), whereas the ν(N–H) has a large red-shift of 131 cm^{-1} for PyWσ. Compared optimized geometry of BzWπ with that of PyWπ, PyWπ shows one H atom of the H_2O molecule to point toward the center of the pyrrole ring while BzWπ shows both H atoms of the H_2O molecule to point toward the benzene ring. In fact, the two "legs" of O–H bonds are not quantmechanically equivalent to each other in BzWπ. To be specific, one O–H bond of water which is closer to benzene ring is elongated by 0.0020 Å while the other O–H bond is elongated by 0.0010 Å relative to its monomer, respectively. A pronounced red-shift of 31 cm^{-1} of the O–H bond of

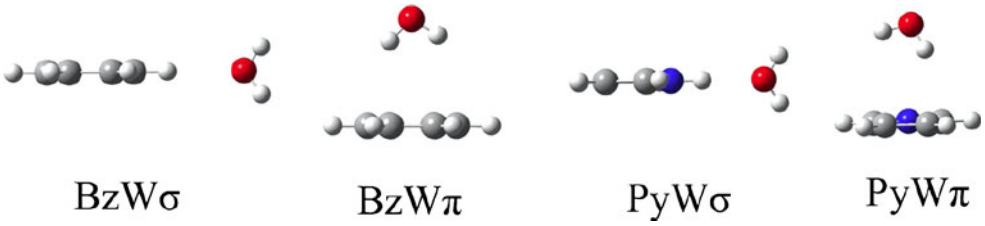

Fig. 1 The optimized geometry at ωb97xD/aug-cc-pVTZ level with BSEE correction

water is observed in BzWπ. In the case of PyWπ, the O–H bond is elongated by 0.0047 Å upon complexation and corresponding red shift is 39 cm^{-1}.

The interaction energies with BSSE correction for BzWσ, PyWσ, BzWπ, and PyWπ are −1.38, −5.27, −3.26 and −4.61 kcal mol^{-1} at the B2PLYPD level which is believed to be a more accurate treatment for noncovalent interactions but more costly computationally [41, 42, 44, 52]. In contrast, the interaction energies from ωb97xD, MP2 and EDA (BLYP-D/TZ2P) methods are similar except that the interaction energy from M06-2X method is slightly different (see Table 2). BzWσ is the least favored with very weak C–H···O interaction while PyWσ is the most favored with strong N–H···O interaction; and the order of interaction energies ΔE is as follows: BzWσ<BzWπ<PyWπ<PyWσ. Overall, pyrrole shows stronger binding energy with water than benzene does when it acts as either the HB acceptor or donor. It indicates that pyrrole has the better ability to form HB with water. This may be one important reason for the different solubility of pyrrole and benzene in water. Moreover, from the ΔE using different methods (see Table 2), the PyWσ is more stable than BzWσ when water acts as the HB acceptor. It may be related to the polarity of C–H and N–H groups in which N–H group is a better HB donor. Meanwhile, the PyWπ is more stable than BzWπ when water acts as HB donor. It is due to the difference in the π electron density in the aromatic ring as HB acceptor. The richer π electron density in the aromatic ring, the better it is as a HB acceptor. It is evident that pyrrole has a more electron-rich π system than benzene, so the former HB is stronger than the latter.

AIM analysis

Bader's topological theory of AIM [54–56] was conducted to analyze these weak interactions. According to the AIM theory, the most important properties include electron densities $\rho(r)_{BCP}$ as well as its Laplacians $\nabla^2\rho(r)_{BCP}$ at the bond critical points (BCPs). The topological parameters for them are listed in Table 3 and BCPs bond paths are shown in Fig. 2.

Although most of O–H···π and C–H···O interactions have been regarded as weak HB, it is still necessary to be confirmed. After all, they are not conventional HBs. As compared with empirical judgments for HB, criteria based on AIM [78, 79] enjoy solid theoretical foundation and good statistical properties. Koch and Popelier proposed eight general topological criteria for existence of HB interactions, of which three are essential and are basically applied [78, 79], namely, i) there exists a bond path between acceptor and donor; ii) the electron density $\rho(r)_{BCP}$ and iii) its Laplacian $\nabla^2\rho(r)_{BCP}$ should be within the ranges of 0.002~0.035 and 0.024~0.139 a.u., respectively. In this paper, the BCPs of the X–H···O interaction between H and O can be found in the BzWσ and PyWσ, which show the BCPs along the bond path joining the H and O atom, as depicted in Fig. 2. For the O–H···π interaction, the BCPs occur between π-aromatic rings and water in the BzWπ and PyWπ, which show the BCPs along the bond path connecting the H atom of water and aromatic ring plane. As for both X–H···O and O–H···π complexes, the values of electron density $\rho(r)_{BCP}$ are in the range of 0.0057~0.022 a.u., and their Laplacian $\nabla^2\rho(r)_{BCP}$ range from 0.017 to 0.084 a.u. (Table 3). Based

Table 1 Geometric characteristics (r or R in Å) and stretching vibrational frequencies ν (cm^{-1}) of X–H bond at ωb97xD/aug-cc-pVTZ with BSSE correction

	BzWσ	PyWσ	BzWπ	PyWπ
ν(C-H)	3208 (−2)			
ν(N-H)		3588 (−131)		
ν(O-H)			3954 (−31)	3946 (−39)
r(C-H)	1.0820 (+0.00031)			
r(N-H)		1.0091 (+0.0078)		
r(O-H)			0.9594 (+0.0020)	0.9621 (+0.0047)
R(O···X)	3.5629	2.9977		
R(O···n1)[a]			3.3085	3.2417
R(X-H···O)	2.4892	1.9888		
R(O-H···n1)[a]			2.7191	2.5090

Values in parenthesis are variations of bond length and frequency shifts of X–H relative to those of the monomers

[a]n1 is the center of mass for pyrrole or benzene ring

Table 2 Comparisons of interaction energy (kcal mol^{-1}) of the complexes calculated by the different methods

	BzWσ	PyWσ	BzWπ	PyWπ
B2PLYPD	−1.38	−5.27	−3.26	−4.61
ωB97xD	−1.18	−5.00	−3.63	−4.74
MP2	−1.35	−5.24	−3.21	−4.44
EDA(BLYP-D)	−1.33	−5.04	−3.39	−4.86
M06-2X	−1.12	−4.95	−3.74	−5.03

All interaction energy calculations with BSSE corrections except for EDA(BLYP-D)

on considerations of variation of bond length, interaction energy and a reference to Popelier's criteria, we hold that the X–H···O and O–H···π interactions can be classified as HB. However, one issue about BzWπ needs to be addressed here (see Fig. 2 and Table 3). For the O–H···π interaction with $\rho(r)_{BCP}$ 0.0069 a.u. in BzWπ, its $\nabla^2\rho(r)_{BCP}$ 0.0021 a.u. is slightly weaker than that of criteria. However, the corresponding *r*(O–H) occurs with significant elongation and rather strong intermolecular interaction energy is found upon complexation. Therefore, it can be appropriate to ascribe this O–H···π interaction to HB. On the other hand, obviously, the O–H···π interaction with $\rho(r)_{BCP}$ 0.0057 a.u. and its $\nabla^2\rho(r)_{BCP}$ 0.017 a.u. in BzWπ falls outside the scope of HB, which should be attributed to van der Waals interaction [80], rather than hydrogen bond.

Grabowski pointed out, the bond paths of BCPs correspond to the preferable interactions which reflect the electron charge distribution [56]. Therefore, for all dimers of this paper, the bond path of BCPs indicates the preferable interaction HB to occur between donor and acceptor. Remarkably, the dimers of σ-type HB are almost exclusively governed by the X–H···O interaction while those of π-type HB are controlled by O–H···π interactions. For the four complexes, the electron density $\rho(r)_{BCP}$ at the BCP has the following order: BzWπ<BzWσ<PyWπ<PyWσ, and the values are 0.0069, 0.0079, 0.011 and 0.022 a.u., respectively. The result shows that there is no linear correlation between the order of $\rho(r)_{BCP}$ and that of the interaction energy Δ*E*.

NBO analysis

Natural bond orbital (NBO) analysis was performed to understand the origins of HB interactions for these clusters. The results are outlined in Table 3.

It is known that hyperconjugative effect plays an important role in the formation of red-shifted HB [60, 81–83], which implies that a certain amount of electron is transferred from HB acceptor to HB donor. Indeed, this is a rearrangement of electron density within each monomer. In the hyperconjugation scheme, the overlap occurs between the vacant molecular orbital of the X–H bond σ*(X–H) and the filled molecular orbital (usually the lone pair LP(Y) or π electronic clouds π(Y)) in the X–H···Y HB. The LP(Y)→σ*(X–H) or π(Y)→σ*(X–H) hyperconjugative interaction caused the red-shifted HB (X–H···Y) because such an interaction leads to an increase of electron density in σ*(X–H). As a result, the X–H bond is weakened and elongated, accompanied by its stretching vibrational frequency shifted to a lower value [81–83]. The strength of the hyperconjugative interaction is closely related to $E^{(2)}$ in the HB interaction. $E^{(2)}$ denotes second-order perturbation energy, which occurred between donor and acceptor of natural bond orbitals. In general, the larger the hyperconjugative effect, the stronger $E^{(2)}$ from the donor to the acceptor [60, 81–83]. Here, as can be seen from Table 3 and Fig. 3, for PyWσ, there is a strong orbital interaction LP(O)→σ*(N–H) and its $E^{(2)}$ is rather great. Compared with PyWσ, BzWσ dimer has a weak orbital interaction LP(O)→σ*(C–H) and its $E^{(2)}$ is moderate. Meanwhile, in the case of π type HB, the hyperconjugative interactions π(Bz)→σ*(O–H) in BzWπ and π(Py)→σ*(O–

Table 3 AIM and NBO analysis of complexes at M06-2X/aug-cc-pVTZ level

	$\rho(r)_{BCP}$[a]	$\nabla^2\rho(r)_{BCP}$[a]	$E^{(2)}$[b]	σ(X-H)[c]	σ*(X-H)[c]
BzWσ	0.0079	0.030	1.16	1.97841 (−0.00121)	0.01469 (+0.0006)
PyWσ	0.022	0.084	7.40	1.98818 (−0.0013)	0.02524 (+0.00927)
BzWπ	0.0057	0.017	0.12		
	0.0069	0.021	0.26	1.99883 (−0.0004)	0.00102 (+0.00102)
PyWπ	0.011	0.034	1.53	1.99899 (−0.00024)	0.00435 (+0.00435)

For the meaning or definition of the parameters see section "AIM analysis" and "NBO analysis" in this manuscript

[a] Values and bond path of BCPs see Fig. 2; All the units are in a.u.

[b] The units are in kcal mol^{-1}

[c] The unit is in *e* for NBO occupancies of σ bonding and σ* anti-bonding orbital in the X–H of the complexes; Values in parenthesis are variations of NBO occupancies relative to those of the monomers

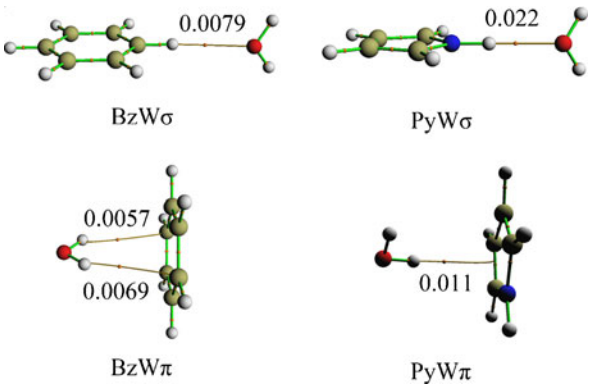

Fig. 2 The molecular graphs for dimers obtained using AIM analysis at M06-2X/aug-cc-pVTZ; the electron density $\rho(r)_{BCP}$ at BCPs, BCPs and its bond path are shown

H) in PyWπ are found, respectively. The magnitude of $E^{(2)}$ values from BzWπ or PyWπ are smaller compared with other conventional HB like the water dimer whose $E^{(2)}$ is 7.60 kcal mol^{-1} at the same calculated level. However, the BzWπ or PyWπ are not yet unstable. The reasons might be due to i) other energy components of weak interaction, for example, van der Waals interaction, also help to stabilizing these clusters. ii) Pyrrole or benzene molecule as HB acceptor have delocalization of large π electronic clouds, which tends to weaken hyperconjugative effect, hence the corresponding $E^{(2)}$ is also decreased.

The NBO occupancy in the bonding σ and anti-bonding σ* orbitals is also a measure of the hyperconjugation effect and strongly related to the bond length and strength. A decrease in σ and an increase in σ* will weaken a bond and thus lead to its elongation, and vice versa [81–83]. As shown in Table 3, for N–H···O HB in PyWσ, the occupancy in the σ*(N–H) orbital has a significant increase and the

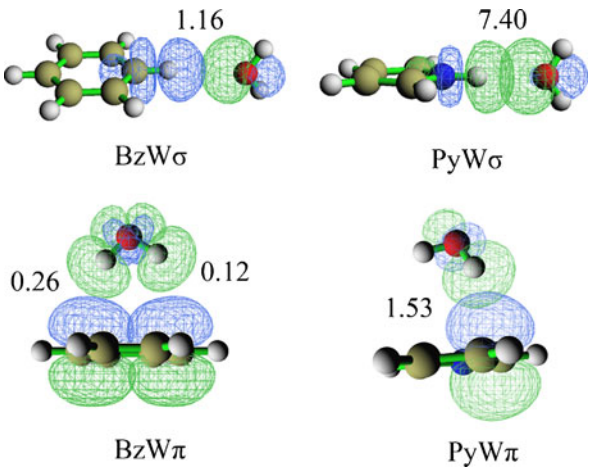

Fig. 3 The molecular graphs for dimers obtained using NBO analysis at M06-2X/aug-cc-pVTZ. The main intermolecular hyperconjugation interactions of LP(O)→σ*(X–H) or π→σ*(X–H) orbitals interaction between two monomers are shown; The values are second-order perturbation energy $E^{(2)}$

occupancy in the σ(N–H) orbital slight decrease with respect to the isolated monomer. The increase of the occupancies in σ*(N–H) is mainly caused by the pairs of intermolecular donor-acceptor orbital interactions such as the LP(O)→σ*(N–H). It is noteworthy that, in the case of C–H···O HB in BzWσ, the occupancy in the σ*(C–H) orbital has a slight increase and that of the σ(C–H) has a moderate decrease relative to the isolated monomer, which results from the occurrence of weak hyperconjugative interaction LP(O)→σ*(C–H). Thus, this LP(O)→σ*(C–H) hyperconjugative interaction is not strong enough to undergo the significant elongation of *r*(C–H), along with a small red-shifted of *ν*(C–H) upon complexation. On the other hand, in the case of O–H···π HBs, two significant increases of occupancies in σ*(O–H) of water were found in BzWπ and PyWπ upon complexation, respectively; while the two occupancies in the σ(O–H) of water decrease slightly with respect to the monomer. The increase of the occupancies in σ*(O–H) is mainly induced by the pairs of intermolecular donor-acceptor orbital interactions such as the π(Py)→σ*(O–H) or π(Bz)→σ*(O–H) (see Fig. 3). In summary, the X–H bond in X–H···O HBs and O–H bond in O–H···π HBs are elongated, accompanied by red-shifts or a small red-shift, which resulted from the hyperconjugations that occurred between acceptor and donor, namely LP(O)→σ*(N–H), LP(O)→σ*(C–H), π(Py)→σ*(O–H) and π(Bz)→σ*(O–H). These results demonstrate that the hyperconjugation effect can be reasonably explained for the origin of the X–H elongation and red-shift (or small red-shift) of these dimers. It seemed that these red-shift HBs are similar in origin, which is either π or σ type.

EDA analysis

To get a better understanding of the nature of the two types of HBs, an energy decomposition analysis (EDA) was carried out at the BLYP-D/TZ2P level of theory, which has been used in the study of the interaction energy for weak interactions [64]. The results of EDA of various aromatic-water clusters and corresponding energy component were listed in Table 4.

The total energies, calculated by means of EDA+BLYP-D/TZ2P, are −1.33, −5.04, −3.39 and −4.86 kcal mol^{-1} for BzWσ, PyWσ, BzWπ and PyWπ, respectively. It is in good agreement with those obtained from B2PLYPD calculations. This indicates that the EDA method can provide reliable energy results for the aromatic-water clusters.

As demonstrated by EDA analysis (Table 4), it is observed easily that the major sources of stabilization of various HB clusters are significantly different. i) For BzWσ and PyWσ of σ type HB, the ΔE_{elstat} dominates over the other two attraction contribution ΔE_{disp} and ΔE_{orb}. In the case of BzWπ, the large contribution to ΔE_{int} comes from the

ΔE_{disp}, rather than ΔE_{elstat}. On the contrary, ΔE_{elstat} of PyWπ is more important than the other attractive energy component. ii) To gain a deeper insight into the dispersion effects among these HBs interactions, we look into the dispersion energy contributions to total interaction energy using the percentage of $\Delta E_{disp}/\Delta E_{int}$. The order of dispersion percentage is BzWπ(~95 %)>PyWπ(~65 %)>BzWσ (~59 %)>PyWσ (~22 %). Clearly, dispersion energy plays an important role in the first three of non-classical HBs while it seems less important in the last of classical HB. No matter in terms of value or percentage, ΔE_{disp} increases significantly for the O–H···π complexes compared with that for X–H···O complexes. It confirms the significance of the dispersion effect on X–H···π interction [4, 5, 39, 40]. iii) Compared with electrostatic and dispersion interactions, orbital interaction ΔE_{orb} may also be an important contribution to stabilizing the clusters and has the same order of magnitude as ΔE_{elstat} or ΔE_{disp}. The order of $\Delta E_{orb}/\Delta E_{int}$ is PyWσ(~66 %)>BzWσ (~54 %)>BzWπ (~52 %)>PyWπ (~51 %), which indicates the effect of intermolecular orbital interactions to have little difference in these dimers.

Liquid mixture of benzene/water and pyrrole/water

X–H···O and O–H···π HBs in liquid mixture

When aromatic-water clusters as gas cluster are expanded to liquid mixture which lacks the well-defined arrangements of basic units (as shown in Fig. 4, where a snapshot of the MD simulation is extracted), the questions arise whether these HB interactions really exist in liquid mixture, and what the exact role it plays in liquid mixture. It is worth keeping in mind that the liquid simulation involving a number of molecules by MD is fundamentally different from the study of clusters involving several molecules by QM, either in terms of calculation methods or results analysis.

MD simulations can be complimentary to experimental observations so that one molecular picture is provided from local structure to weak interaction at atom level. For liquid mixture of benzene/water or pyrrole/water, most previous works [14, 15, 25–32] have analyzed the local structure, hydrophobic effect and the orientation of interfacial water or interfacial aromatics in diluted solution. Here, we presented a detail analysis of local structure of the various types of HBs which occurred in 1:1 mixture of benzene/water and pyrrole/water under ambient conditions. As a reflection on these cluster models (Bz:W=1:1, Py:W=1:1), we believe our simulation of liquid models are more appropriate to reproduce the actual system compared with infinite diluted solution. The different types of HBs existing in binary liquid mixtures of aromatics and water under ambient conditions deserved more attention because they are close to the practical interactions like chemical, physical, and biological processes. Meanwhile, liquid mixture was further simulated at 278 K, 298 K and 318 K because we can observe how the temperature affects the σ and π HB in liquid mixture.

Table 4 Energy decomposition analysis at BLYP-D/TZ2P (kcal mol^{-1})

	ΔE_{int}	ΔE_{elstat}	ΔE_{pauli}	ΔE_{orb}	ΔE_{disp}
BzWσ	−1.33	−1.60	1.79	−0.72	−0.79
PyWσ	−5.04	−7.31	6.71	−3.34	−1.10
BzWπ	−3.39	−2.62	4.21	−1.77	−3.21
PyWπ	−4.86	−4.57	5.35	−2.50	−3.15

$\Delta E_{int} = \Delta E_{elstat} + \Delta E_{disp} + \Delta E_{pauli} + \Delta E_{orb}$

Snapshots of the solution structures of liquid mixture for the benzene/water and pyrrole/water are given in Fig. 4, which was extracted from MD simulations. Although they show instantaneous arrangements in the solution, they are still representative of some interesting findings. The snapshots show that aromatic and water molecules are not randomly distributed. The observations tally with the fact that benzene or pyrrole did not dissolve easily in water. Moreover, we also observe that various molecular contacts such as O–H···π or X–H···O occurred between molecules.

However, the pyrrole/water and benzene/water mixtures present different behaviors. For pyrrole/water, most of the water molecules move as a self-aggregated cluster in the pyrrole molecules like some kind of a microemulsion of water-in-oil. At the same time, a few isolated water molecules can leak into the bulk of pyrrole molecules. The snapshot of pyrrole/water mixture indicates that a rather strong attractive force existed between unlike molecules in this mixture. In contrast, the snapshot of liquid mixture benzene/water clearly shows that the separation between the water and benzene liquid phases is well defined and that almost no water was found in the benzene bulk, which indicates that no strong attraction existed between unlike molecules in this mixture. These findings are further analyzed by the RDFs profiles related to the HBs.

To analyze in more detail how the HBs take place between aromatic molecular and water, we calculate various inter-atomic distribution functions. A standard method of studying the structure of liquid or solution is to calculate RDFs between different interaction sites. These quantities are known as "pair correlation functions" and denoted as "$g(r)$[X···Y]", which gives the probability of finding a particle of type Y at a distance r from a particle of type X relative to average probability [69]. The interaction O–H···π can be appropriately simplified by computing the atom H attached to O–H group of water and n1 pair distribution $g(r)$[O–H···n1], n1 being the center of mass for pyrrole or benzene. Meanwhile, the X–H···O interaction can also be intuitively expressed by computing the pair distribution $g(r)$[N–H···O] or $g(r)$[C–H···O].

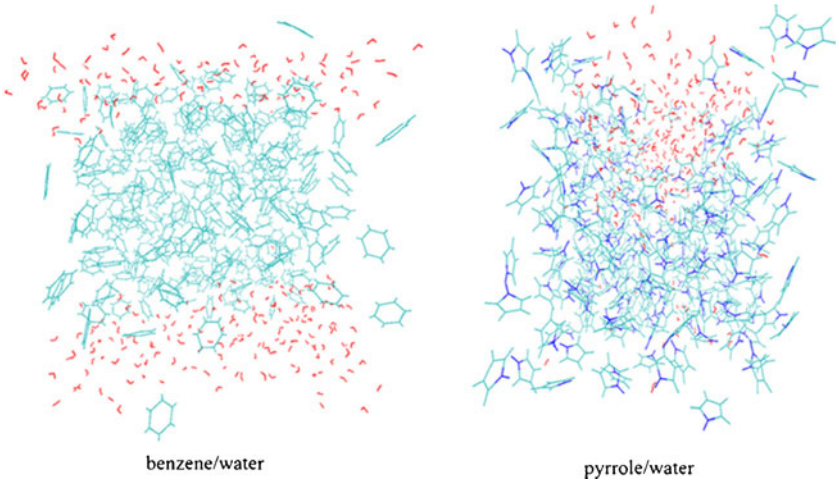

Fig. 4 Snapshot of the liquid mixture extracted from the MD simulations

The occurrence of the distinct peaks $g(r)$[X···Y] implies that the particle pairs are orderly assembled and the amplitude of the peaks reflects the contact strength of particle pairs [69]. Figure 5 shows $g(r)$[C–H···O] and $g(r)$[N–H···O] of aromatic-water at different temperatures, respectively. As expected, $g(r)$[N–H···O] of the liquid mixture of pyrrole/water showed significant peaks near 1.9 Å [15], indicating formation of the N–H···O ordered assembly. From the amplitude of the peak, it is evident that strong N–H···O HB was formed in its liquid mixture [15]. Note that the peaks at ca. 1.9 Å are close to the r(N–H···O) resulted from PyWσ (1.9888 Å) optimized by QM. In the case of C–H···O HB in liquid mixture of benzene/water, beyond our expectations, no well-defined peaks were found in the range of HB, which is totally different from the case of $g(r)$[N–H···O]. In other words, the peaks completely disappeared in the range from 1.2 to 3.0 Å which is generally regarded as the general distance of HB between donor and acceptor [84]. It is therefore concluded that the C–H···O order assembly is very difficult or even impossible to be yielded as HB manner in liquid mixture benzene/water. This observation from MD results reflects that C–H···O local structure can not form practical contacts, which is in agreement with the result of BzWσ from QM. In QM calculation, BzWσ involving C–H···O weak interaction is believed to be the least stable of four dimers.

As for O–H···π interactions (see Fig. 6), it is seen that they exhibited the first peak located at 2.3 Å for liquid mixture of pyrrole/water and 2.4 Å for liquid mixture of benzene/water, respectively. Both of peaks are close to the r (O–H···π) resulted from PyWπ (2.5090 Å) and BzWπ (2.7191 Å) optimized by QM, respectively. The occurrence of two peaks indicates that the regular assembly existed between H atom of water and aromatic ring in the liquid mixture aromatic/water. The peak amplitudes of $g(r)$[O–H···π] are not high, which demonstrate that the H atoms of water occasionally but still regularly come close to the benzene or pyrrole ring region (or we can regard it as relative contacts). The results confirm that such O–H···π HBs exist in liquid mixture of benzene/water and pyrrole/water. In particular, O–H···π pair interactions are found to dominate in liquid mixture benzene/water [25, 26, 30, 31], rather than liquid mixture pyrrole/water. According to the configuration of BzWπ and Allesch's viewpoint [31], this O–H···π interaction occurred between π plane of benzene and O–H bond of water molecule in liquid mixture benzene/water, and this region perpendicular to the π plane is termed as hydrophilic region [31].

Not surprisingly, the strength of $g(r)$[O–H···π] is weaker than that of $g(r)$[N–H···O], reflecting the O–H···π HB is relatively weak in the liquid mixture. Clearly, the order of the strength of various HBs in liquid mixture of aromatic/water is the following: N–H(Py)···O(W) > O–H(W)···π(Py) > O–H(W)···π(Bz), which is consistent with the order of the interaction energy from QM.

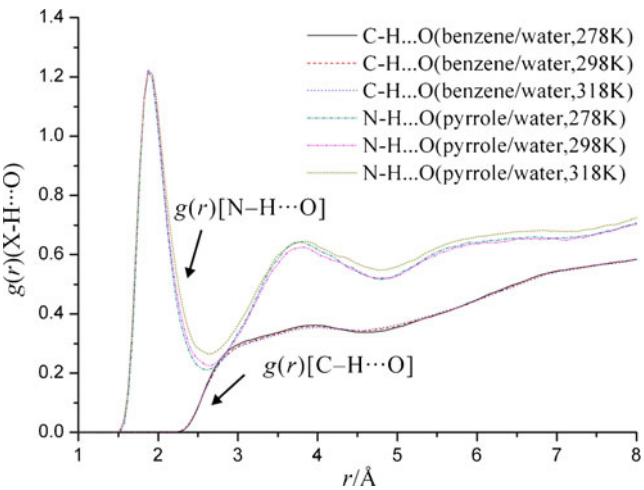

Fig. 5 RDFs for $g(r)$[C–H···O] in liquid mixture of benzene/water and RDFs for $g(r)$[N–H···O] in liquid mixture of pyrrole/water at different temperatures

Moreover, it is interesting to note that the intensity of three types of HBs showed no significant variation at the temperatures of 278 K, 298 K and 318 K. As we know, one important characteristics of HB is that it tends to break with increasing temperature. However, such characteristics were not observed in our simulation results. Then, how does temperature affect the formation of these HBs? We think that the influence of increasing temperature on HB has two opposite effects. On the one hand, owing to its poor solubility in water, the solubility of aromatic in water tends to increase when the temperature rises. As a result, more HBs are likely to form because more aromatic can visit the water bulk with increased temperature. On the other hand, increasing temperature leads to breaking HB already formed in the liquid mixture. Both effects act simultaneously and cancel each other out, hence leading to eventually no significant variation of HB strength when the temperature varies.

Explanation of different solubility of aromatic compounds in water

It should be pointed out that the solvation of aromatic by water is a complicated process and might be influenced by multiple factors such as HB, van der Waals force, hydrophobic effect [85, 86]. HB, as a strong directional force between unlike molecules in the binary liquid mixture, is doubtless one of the most important factors in soluble behaviors. The analysis of the HB strength that occurred between aromatic moiety and water in liquid mixture can help explain different solubility. Based on the above analysis of liquid mixture of aromatic/water and of clusters of aromatic-water, we would like to draw attention to the difference in solubility of benzene in water (1.77 g (benzene)/1 kg(water) at 20 °C, 1.83 g (benzene)/1 kg(water) at 30 °C) and pyrrole in water (47 g(pyrrole)/1 kg(water) at 25 °C) [87]. On the one hand, snapshots illustrate that the pyrrole is easier to dissolve in water than benzene. Meanwhile, RDFs in our cases show that strengths of different types of HB in pyrrole/water mixture are greater than that in benzene/water mixture at room temperature. On the other hand, the HB interaction energy of pyrrole-water clusters is also larger than that of benzene-water cluster, either as σ type or as π type. Herein, from the point of HB contribution, it well accounts for the difference in solubility of benzene and pyrrole in water. However, our study is limited to the HB effect without considering the hydrophobic effect, which remains challenging for future work.

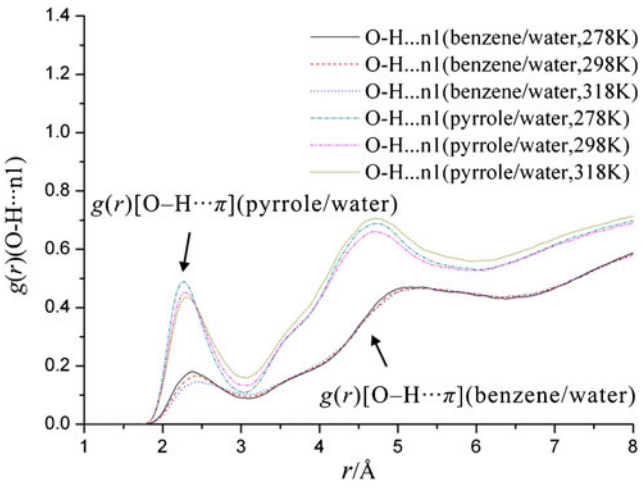

Fig. 6 RDFs for $g(r)$[O–H···n1] in liquid mixture of benzene/water and RDFs for $g(r)$[O–H···n1] in liquid mixture of pyrrole/water at different temperatures; n1 is the center of mass for pyrrole or benzene molecules

Conclusions

Benzene-water and pyrrole-water are among the often studied aromatic-water models due to their interesting small structure and various inter-molecular contacts. The focus of this study is the similarity and difference of two types of HB between benzene-water as well as pyrrole-water, respectively. The two types of HBs, namely, the X–H···O σ type and the O–H···π π type, as identified in the clusters of benzene-water and pyrrole-water, were investigated by high-level QM. Meanwhile, classical MD was applied to the study of the same HBs existing in the two liquid mixtures of benzene/water (1:1) and pyrrole/water (1:1), which correspond to their clusters.

The ωb97xD including dispersion correction term with aug-cc-pVTZ basis set was chosen to determine the geometries of the X–H···O σ and the O–H···π π HB. The order of interaction energy is PyWσ>PyWπ>BzWπ>BzWσ at different calculated levels. In additional, three obvious red-shifted HBs and one small red-shift HB were observed in these dimers. The AIM analysis provides the supports for the existence of X–H···O and the O–H···π HB. From the NBO analysis, it becomes evident that the origin of red-shifted HBs can be explained by the hyperconjugation model (LP (O)→σ*(X–H) or π(Bz/Py)→σ*(O–H)) during the HB formation processes. The EDA investigations imply that the HBs of σ and π are controlled by quite different energy components. The above results can shed some light on the nature of the σ and the π type HBs in benzene-water and pyrrole-water clusters, which can help us to further investigate the local structure and similar HBs for benzene/water and pyrrole/water in liquid phase. Our MD simulation results show the different local structure and strength for these HBs in the liquid mixtures, which are somewhat different but reasonable for the clusters by QM. Furthermore, we explain the difference in solubility of benzene and pyrrole in water resulted from MD and QM.

This study will lead to a deeper understanding of the local structure and intermolecular interaction between aromatic and water, and will provide reasonable exploration of experimental results for other similar systems. The theoretical investigation of another heterocyclic and its mixtures is currently in progress in our group.

Acknowledgments Financial support by the National Natural Science Foundation of China (No. 21173069) as well as the Science and Technology Foundation of Guangdong Province, China (2010B060900084) are acknowledged. Authors also thank Dr. Tian Lu at the Institute of Chemical and Biological Technology, University of Science and Technology Beijing for helpful discussion. The computation of the Gaussian is supported by the School of Chemical and Environmental Sciences, Henan Normal University.

References

1. Mata I, Alkorta I, Molins E, Espinosa E (2010) Chem Eur J 16:2442–2452
2. Tsuzuki S, Uchimaru T (2006) Curr Org Chem 10:745–762
3. Scheiner S, Kar T, Pattanayak J (2002) J Am Chem Soc 124:13257–13264
4. Riley KE, Pitoňák M, Černý J, Hobza P (2010) J Chem Theory Comput 6:66–80
5. Donoso-Tauda O, Jaque P, Santos JC (2011) Phys Chem Chem Phys 13:1552–1559
6. Tsuzuki S, Fujii A (2008) Phys Chem Chem Phys 10:2584–2594
7. Tsuzuki S, Honda K, Uchimaru T, Mikami M, Tanabe K (2000) J Am Chem Soc 122:11450–11458
8. Meyer EA, Castellano RK, Diederich F (2003) Angew Chem Int Ed 42:1210–1250
9. Hobza P, Müller-Dethlefs K (2010) Non-covalent interactions: theory and experiment. RSC, Cambridge
10. Carles S, Lecomte F, Schermann JP, Desfrançáois C (2000) J Phys Chem A 104:10662–10668
11. Maris A, Melandri S, Miazzi M, Zerbetto F (2008) ChemPhysChem 9:1303–1308
12. Crittenden DL (2009) J Phys Chem A 113:1663–1669
13. Mishra BK, Sathyamurthy N (2007) J Phys Chem A 111:2139–2147
14. Schwartz CP, Uejio JS, Duffin AM, England AH, Prendergast D, Saykally RJ (2009) J Chem Phys 131:114509
15. Nagy PI, Durant GJ, Smith DA (1993) J Am Chem Soc 115:2912–2922
16. Janjić GV, Veljković DŽ, Zarić SD (2011) Cryst Growth Des 11:2680–2683
17. Suzuki S, Green PG, Bumgarner RE, Dasgupta S, Goddard WA III, Blake GA (1992) Science 257:942–945
18. Augspurger JD, Dykstra CE, Zwier TS (1993) J Phys Chem 97:980–984
19. Tarakeshwar P, Choi HS, Lee SJ, Lee JY, Kim KS, Ha T-K, Jang JH, Lee JG, Lee H (1999) J Chem Phys 111:5838–5850
20. Prakash M, Samy KG, Subramanian V (2009) J Phys Chem A 113:13845–13852
21. Feller D (1999) J Phys Chem A 103:7558–7561
22. Ma J, Alfè D, Michaelides A, Wang E (2009) J Chem Phys 130:154303
23. Li S, Cooper VR, Thonhauser T, Puzder A, Langreth DC (2008) J Phys Chem A 112:9031–9036
24. Slipchenko LV, Gordon MS (2009) J Phys Chem A 113:2092–2102
25. Gierszal KP, Davis JG, Hands MD, Wilcox DS, Slipchenko LV, Ben-Amotz DJ (2011) J Phys Chem Lett 2:2930–2933
26. Raschke TM, Levitt M (2004) J Phys Chem B 108:13492–13500
27. Keresztúri Á, Jedlovszky P (2005) J Phys Chem B 109:16782–16793
28. Ikawa S-I (2005) J Chem Phys 123:244507
29. Gamieldien MR, Strümpfer J, Naidoo KJ (2012) J Phys Chem B 116:324–331
30. Allesch M, Lightstone FC, Schwegler E, Galli G (2008) J Chem Phys 128:014501
31. Allesch M, Schwegler E, Galli G (2007) J Phys Chem B 111:1081–1089
32. Urahata S, Canuto S (1999) Chem Phys Lett 313:235–240
33. Tubergen MJ, Andrews AM, Kuczkowski RL (1993) J Phys Chem 97:7451–7457
34. Matsumoto Y, Honma K (2009) J Chem Phys 130:054311
35. Li Y, Liu X-H, Wang X-Y, Lou N-Q (1999) J Phys Chem A 103:2572–2579
36. Kumar A, Kołaski M, Kim KS (2008) J Chem Phys 128:034304
37. Sobolewski AL, Domcke W (2000) Chem Phys Lett 321:479–484
38. Frank I, Damianos K (2008) Chem Phys 343:347–352
39. Riley KE, Pitoňák M, Jurečka P, Hobza P (2010) Chem Rev 110:5023–5063
40. Hohenstein EG, Sherrill CD (2009) J Phys Chem A 113:878–886
41. Grimme S, Antony J, Ehrlich S, Krieg H (2010) J Chem Phys 132:154104
42. Goerigk L, Grimme S (2011) Phys Chem Chem Phys 13:6670–6688
43. Grimme S (2011) WIREs Comput Mol Sci 1:211–228
44. Burns LA, Vázquez-Mayagoitia Á, Sumpter BG, Sherrill CD (2011) J Chem Phys 134:084107
45. Chai J-D, Head-Gordon M (2008) Phys Chem Chem Phys 10:6615–6620
46. Chai J-D, Head-Gordon M (2008) J Chem Phys 128:084106
47. Tian B, Eriksson ESE, Eriksson LA (2010) J Chem Theory Comput 6:2086–2094
48. Kang YK, Byun BJ (2010) J Comput Chem 31:2915–2923
49. Simon S, Duran M (1996) J Chem Phys 105:11024–11031
50. Boys SF, Bernardi F (1970) Mol Phys 19:553–566
51. Frisch MJ, Trucks GW, Schlegel HB, Scuseria GE, Robb MA, Cheeseman JR et al. (2010) Gaussian 09 C01. Gaussian Inc, Wallingford, CT. <http://www.gaussian.com>
52. Schwabe T, Grimme S (2007) Phys Chem Chem Phys 9:3397–3406
53. Zhao Y, Truhlar DG (2008) Acc Chem Res 41:157–167
54. Bader RFW (1991) Chem Rev 91:893–928
55. Bader RFW (1990) Atoms in molecules: a quantum theory. Clarendon, Oxford
56. Grabowski SJ, Ugalde JM (2010) J Phys Chem A 114:7223–7229
57. Keith TA, AIMAll, Version 10.03.25, <http://aim.tkgristmill.com>
58. Lu T, Chen F (2012) J Comput Chem 33:580–592
59. Lu T. Multiwfn, Version 2.3.3, <http://multiwfn.codeplex.com>
60. Reed AE, Curtiss LA, Weinhold F (1988) Chem Rev 88:899–926
61. Morokuma K (1971) J Chem Phys 55:1236–1244
62. Ziegler T, Rauk A (1977) Theor Chim Acta 46:1–10
63. Mitoraj MP, Michalak A, Ziegler T (2009) J Chem Theory Comput 5:962–975
64. Grimme S, Antony J, Schwabe T, Mück-Lichtenfeld C (2007) Org Biomol Chem 5:741–758
65. Baerends EJ, Autschbach J, Bashford D, Bérces A, Bickelhaupt FM, Bo C et al (2012) ADF version 2012.01, SCM, Theoretical Chemistry, Vrije Universiteit, Amsterdam, The Netherlands.<http://www.scm.com>
66. te Velde G, Bickelhaupt FM, Baerends EJ, Fonseca Guerra C, van Gisbergen SJA, Snijders JG, Ziegler T (2001) J Comput Chem 22:931–967
67. Bickelhaupt FM, Baerends EJ (2000) Kohn-Sham density functional theory: predicting and understanding chemistry. In:

Lipkowitz KB, Boyd DB (eds) vol. 15 Rev Comput Chem. Wiley-VCH, New York, pp 1–86 doi:10.1002/9780470125922.ch1
68. Liu Z (2009) J Phys Chem A 113:6410–6414
69. Allen MP, Tildesley DJ (1987) Computer simulation of liquids. Clarendon, Oxford
70. Jorgensen WL, Maxwell DS, Tirado-Rives J (1996) J Am Chem Soc 117:11225–11236
71. Ponder JW. Tinker, version 4.2, <http://dasher.wustl.edu/tinker>
72. Mark P, Nilsson L (2001) J Phys Chem A 105:9954–9960
73. Berweger CD, van Gunsteren WF, Müller-Plathe F (1995) Chem Phys Lett 232:429–436
74. McDonald NA, Jorgensen WL (1998) J Phys Chem B 102:8049–8059
75. Cornell WD, Cieplak P, Bayly CI, Gould IR, Merz KM, Ferguson DM, Spellmeyer DC, Fox T, Caldwell JW, Kollman PA (1995) J Am Chem Soc 117:5179–5197
76. Joseph J, Jemmis ED (2007) J Am Chem Soc 129:4620–4632
77. Pluháčková K, Hobza P (2007) ChemPhysChem 8:1352–1356
78. Koch U, Popelier PLA (1995) J Phys Chem 99:9747–9754
79. Lipkowski P, Grabowski SJ, Robinson TL, Leszczynski J (2004) J Phys Chem A 108:10865–10872
80. Johnson ER, Keinan S, Mori-Sánchez P, Contreras-García J, Cohen AJ, Yang W (2010) J Am Chem Soc 132:6498–6506
81. Chocholoušová J, Špirko V, Hobza P (2004) Phys Chem Chem Phys 6:37–41
82. Alabugin IV, Manoharan M, Peabody S, Weinhold F (2003) J Am Chem Soc 125:5973–5987
83. Zhou P-P, Qiu W-Y (2009) J Phys Chem A 113:10306–10320
84. Rozas I (2007) Phys Chem Chem Phys 9:2782–2790
85. Raschke TM, Levitt M (2005) Proc Natl Acad Sci U S A 102:6777–6782
86. Chandler D (2005) Nature 437:640–647
87. Lide DR (ed) (2010) CRC handbook of chemistry and physics, 90th edn., (internet version 2010). CRC Press/Taylor and Francis, Boca Raton